



A SIMPLE GEOMETRICAL INDEX CHARACTERIZING GROUND MOTIONS IN VARIOUS SHAPES OF ALLUVIAL VALLEYS

Satoshi MATSUDA¹, Masahiro KAWANO² and Koichiro ASANO³

SUMMARY

The purpose of this study is to propose a simple geometrical index that characterizes the ground motions in various shapes of alluvial valleys. We introduce and define an equivalent flat layer model of an alluvial valley with respect to the dispersion characteristics of surface waves. The thickness of the equivalent flat layer is proposed as a new simple index to quantify the degree of geometrical irregularities and their influence on ground motions. Fundamental examinations for two- and three-dimensional alluvial valleys with simple configurations show the potential utility of newly introduced index to characterize ground motions in alluvial valleys.

INTRODUCTION

Geological lateral irregularities such as alluvial valleys may induce localized large amplifications of ground motions during earthquakes. Bard [1,2] pointed out that locally generated surface waves play an important role to characterize the response of alluvial valleys. The features of surface waves and consequent surface amplifications of alluvial valleys depend greatly on the valley shape, the velocity contrast, and the incident wave field. Their wide and complex variations make difficult to describe generally the influence of various geological irregularities on ground motions.

The purpose of this study is to propose a simple geometrical index that characterizes the ground motions in various shapes of alluvial valleys. We introduce and define an equivalent flat layer model of an alluvial valley with respect to the dispersion characteristics of surface waves. Using the thickness of the equivalent flat layer, we attempt to quantify the degree of irregularity of alluvial valleys. As fundamental study, the equivalent thicknesses are calculated for two- and three-dimensional models of alluvial valleys with simple configurations. Through some examinations, we estimate the potential utility of the newly introduced geometrical index to characterize the ground motions in various shapes of alluvial valleys.

¹ Lecturer, Kansai University, Osaka, Japan. Email: matsuda@ipcku.kansai-u.ac.jp

² Former Professor, Kyoto University, Kyoto, Japan.

³ Professor, Kansai University, Osaka, Japan.

RESPONSE TIME HISTORIES OF ALLUVIAL VALLEYS FOR INCIDENT SH, P, AND SV WAVES

Figure 1 shows the two-dimensional (2D) and three-dimensional (3D) models of alluvial valleys to be analyzed in this study. An alluvial valley consists of an elastic half-space R_0 and a soft elastic inclusion R_1 . The material properties in R_0 are given by the mass density ρ_0 , the shear rigidity μ_0 , and the Poisson's ratio ν_0 . The material properties in R_1 are designated by subscript 1. Two geometrical types of alluvial valleys are considered in 2D analysis; one is a half-ellipse referred to as E(2D), and another is a half-cycle cosine referred to as C(2D). For each model, two shape ratios $b/a=1/2$ and $1/4$ are considered, where a is the half-width of the valley and b is the maximum depth. In 3D analysis, two types of axi-symmetric valleys E(3D) and C(3D) are considered. Each of them has the same vertical section as the corresponding 2D model. Two sets of material properties are assumed; for the hard model (low velocity contrast): $\rho_1/\rho_0=1.0$, $\mu_1/\mu_0=0.2$, $\nu_0=0.25$, $\nu_1=0.30$, and for the soft model (high velocity contrast): $\rho_1/\rho_0=1.0$, $\mu_1/\mu_0=0.1$, $\nu_0=0.25$, $\nu_1=0.30$.

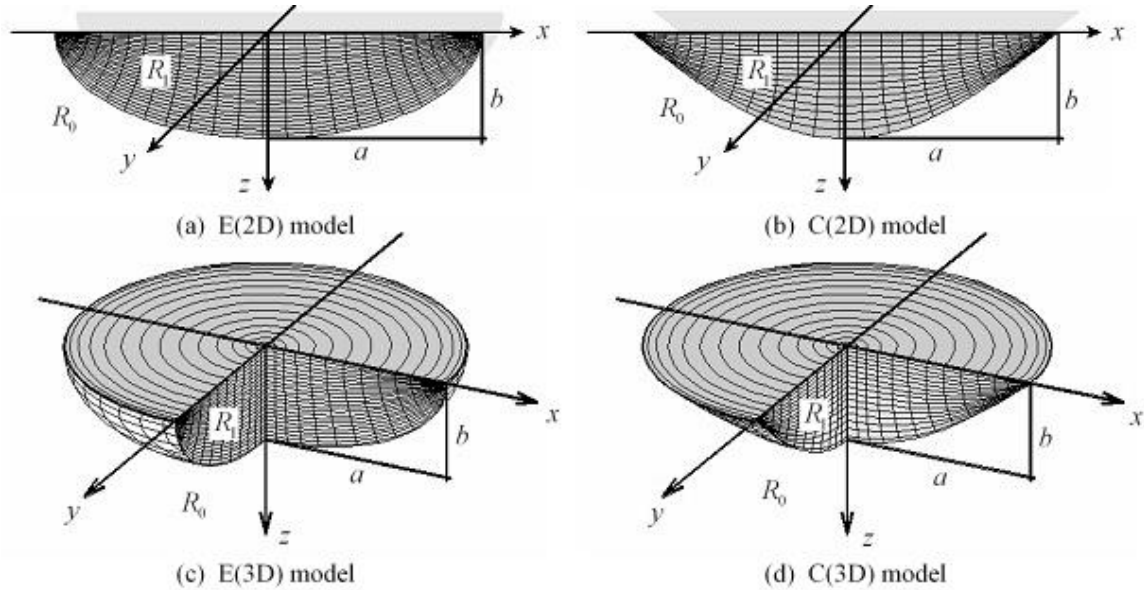
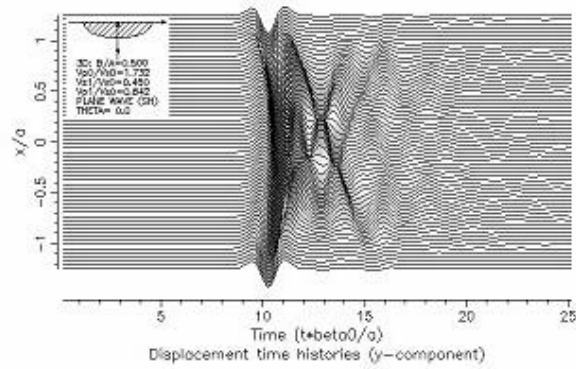


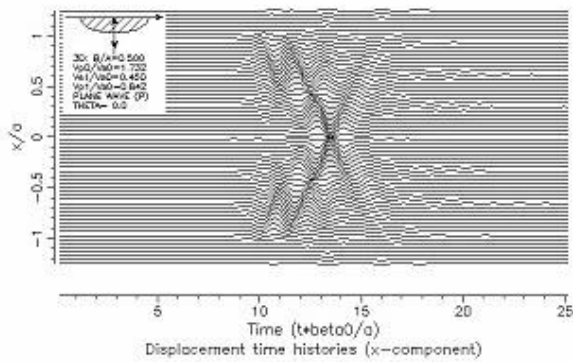
Figure 1. 2D and 3D alluvial valley models

The ground motions under incident plane SH, P, and SV waves were calculated by using a hybrid method of the Riccati equation approach (Marsh [3]) for the elastic wave fields in R_1 and the direct BEM for R_0 . In generalized coordinates conforming to the boundary shape of the alluvial valley, we expressed the wave fields in R_1 by means of “up-going” and “down-going” propagator matrices and impose the boundary conditions at the R_0 - R_1 interface using the Somigliana integral equation (Matsuda [4]). Through the discretization of the boundary, wave field solutions are computed in the frequency domain. Time domain solutions are synthesized by using the FFT algorithm.

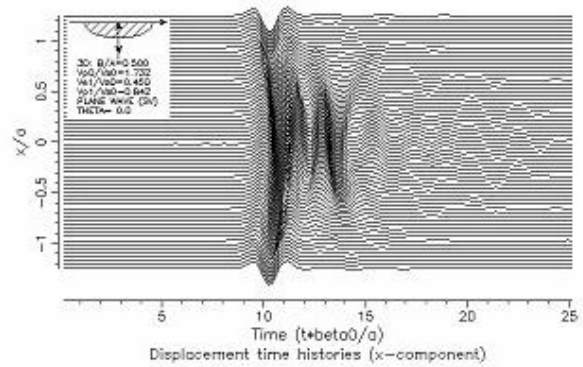
As numerical examples, Fig. 2 shows the displacement time histories of the hard E(3D) model with $b/a=1/2$ at the receivers along the x -axis under vertical incidence of plane SH waves (corresponding to the disturbance in the y -direction), P waves (in the z -direction), and SV waves (in the x -direction). The incident time function was given by the Ricker wavelet with the characteristic period of $t_c=2a/\beta_0$, where β_0 denotes the shear wave velocity in R_0 . In Fig. 2, the horizontal time axis (t) is scaled by a/β_0 , and the vertical axis (x) is scaled by a (then the values ± 1 correspond to the valley edges).



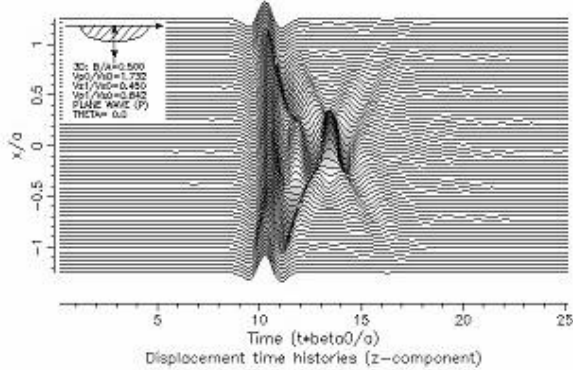
(a) vertical incidence of plane SH waves



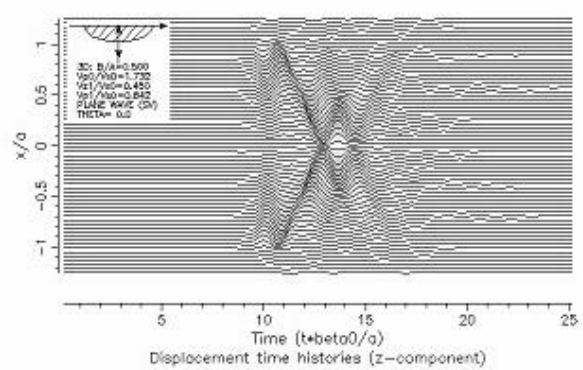
Displacement time histories (x-component)



Displacement time histories (x-component)



Displacement time histories (z-component)



Displacement time histories (z-component)

(b) vertical incidence of plane P waves

(c) vertical incidence of plane SV waves

Figure 2. Displacement time histories of the hard E(3D) model

In this figure, it is observed that the first direct waves are followed by surface waves generated at the valley edges and propagating laterally to the other edges. For the cases of incident P and SV waves, the surface waves appear rather clearly in the z -component. Later phases with relatively large amplitudes are observed at the central region of the alluvial valley in the z -component for incident P waves and in the x -component for incident SV waves. They are probably because of the symmetric properties of the disturbances and the valley's shape. The disturbances are axi-symmetric for vertical incidence of P waves, so that the surface waves arrive at the same time and in phase at the center of the valley. For vertical incidence of SV waves, the disturbances are symmetric about the x - z plane, so that the surface waves meet in phase at the points on the x -axis.

EQUIVALENT FLAT LAYER MODEL

Figure 3 shows the contour maps of the displacement amplitude in the $\omega-k_x$ (circular frequency-wavenumber in the x -direction) domain plotted on the $\omega-\omega/k_x$ plane for the same cases shown in Fig. 2. The vertical axis (ω/k_x) scaled by β_0 indicates the phase velocity in the positive x -direction. The horizontal axis (ω) is scaled by β_0/a . The dispersion characteristics of the surface waves generated in the alluvial valley are observed from the trains of peaks in Fig. 3. The phase velocity varies from about β_0 to β_1 ($<\beta_0$) as the frequency increases, where β_1 denotes the shear wave velocity in the alluvial valley.

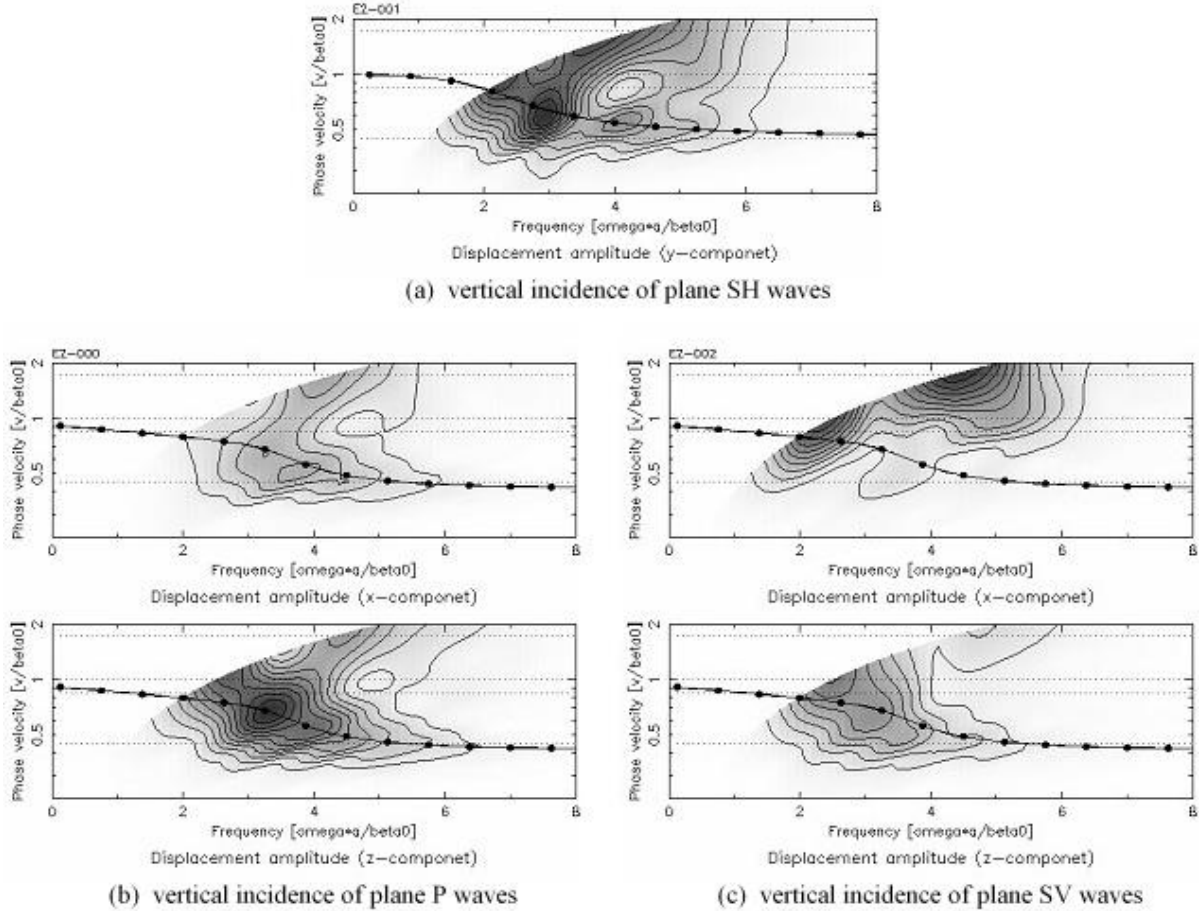


Figure 3. Displacement amplitudes in the frequency-wavenumber domain and dispersion curves

Here, we introduce an equivalent flat layer model: a single flat layer overlying a half-space with the same velocity contrast as the alluvial valley model. The thickness Heq of the equivalent flat layer is determined so that the theoretical dispersion curve of the fundamental Love or Rayleigh wave in the flat layer fits best to the one in the alluvial valley estimated from the $\omega-\omega/k_x$ diagram by using the least squares fitting technique. For the cases of incident SH waves, the surface waves generated in the alluvial valleys are assumed to be Love waves. In Fig. 3(a), the theoretical dispersion curve of the fundamental Love wave in the flat layer with the thickness Heq is plotted by a solid symbol line. The fundamental Rayleigh waves are assumed for the cases of incident P and SV waves. The equivalent thickness Heq is estimated from the $\omega-\omega/k_x$ diagram of the z -component, in which the surface waves are rather distinct. Within the range of this analysis, the difference is small between the equivalent thicknesses estimated from the P and SV

waves incidence. The theoretical dispersion curve of the fundamental Rayleigh wave in the equivalent flat layer model are also plotted in Fig. 3(b) and (c).

Table 1 and 2 list the Heq estimated from the 2D and 3D analyses, respectively, where we can obtain common properties of the Heq in 2D and 3D as follows. (1) The Heq/b is less than unity, i.e., the Heq is smaller than the maximum depth of the valley. (2) The Heq for Love waves is smaller than that for Rayleigh waves. (3) The Heq for the type C (a half-cycle cosine) model is small compared to that for the type E (a half-ellipse) model with the same b/a . (4) The Heq/b for $b/a=1/4$ is smaller than that for $b/a=1/2$. The average depth of the alluvial valley is proportional to the maximum depth b for all the models in this analysis: $(\pi/4)b=0.785b$ for E(2D), $(2/\pi)b=0.637b$ for C(2D), $2b/3=0.667b$ for E(3D), and $4(\pi-2)b/\pi^2=0.463b$ for C(3D). Contrary to our ordinary expectation, the obtained Heq is not proportional to b . (5) The Heq for the 3D model is smaller than that for the corresponding 2D model. There is no exception, at least in Table 1 and 2, to the rules governing Heq mentioned above. The difference between the equivalent thicknesses for the hard and soft models seems to be small, and we cannot find any simple relations. Taking into account of errors coming from the fitting process, it seems that the Heq might be more strongly governed by the geometrical properties of the alluvial valley than by the material properties.

Table 1 . The thickness of the equivalent flat layer model estimated from the 2D analysis

Shape		E(2D)		C(2D)		E(2D)		C(2D)	
Depth (b/a)		1/2	1/4	1/2	1/4	1/2	1/4	1/2	1/4
Material property		Hard				Soft			
Love wave	Heq/a	0.340	0.192	0.317	0.189	0.331	0.200	0.301	0.189
	Heq/b	0.679	0.770	0.633	0.755	0.663	0.801	0.602	0.755
Rayleigh wave	Heq/a	0.378	0.235	0.370	0.220	0.393	0.227	0.378	0.220
	Heq/b	0.775	0.939	0.740	0.878	0.786	0.908	0.755	0.878

Table 2. The thickness of the equivalent flat layer model estimated from the 3D analysis

Shape		E(3D)		C(3D)		E(3D)		C(3D)	
Depth (b/a)		1/2	1/4	1/2	1/4	1/2	1/4	1/2	1/4
Material property		Hard				Soft			
Love wave	Heq/a	0.278	0.170	0.232	0.154	0.286	0.174	0.248	0.162
	Heq/b	0.556	0.679	0.464	0.617	0.571	0.694	0.495	0.648
Rayleigh wave	Heq/a	0.317	0.208	0.301	0.185	0.332	0.208	0.301	0.197
	Heq/b	0.633	0.832	0.602	0.740	0.663	0.832	0.602	0.786

DISCUSSION

As the thickness Heq decrease, the Airy-phase frequency in the equivalent flat layer shifts toward a higher frequency. Therefore, the frequency range lower than the Airy-phase frequency becomes wider, within which the surface flat layer and the half-space move “in phase” with the phase velocity close to that for the half-space. From this theoretical viewpoint, the equivalent thickness Heq of an alluvial valley defined in this study could give a measure of the constraints imposed by the surrounding half-space. The smaller Heq means the stronger constraints. Therefore, the smaller Heq for the type C valley than that for the type E valley is interpreted as the stronger constraints to the type C valley probably because of its relative shallowness and the gentle slope of its shoulders.

The surface waves generated in the alluvial valley induce some complicated patterns in the spatial distribution of amplifications. Figure 4 shows the contour maps of the surface amplifications in the $x-\omega$

domain. Figure 4(a) is that of the hard E(3D) model for vertical incidence of SH waves (corresponding to the case shown in Fig. 2(a)), and Fig. 4(b) is that for the oblique incidence making an angle of 30° with the positive z -axis and traveling in the x - z plane. The number of peaks in space grows with the frequency, but large amplifications concentrate gradually in the central region of the alluvial valley. For case of the oblique incidence, large amplifications shift toward the opposite side to the incidence.

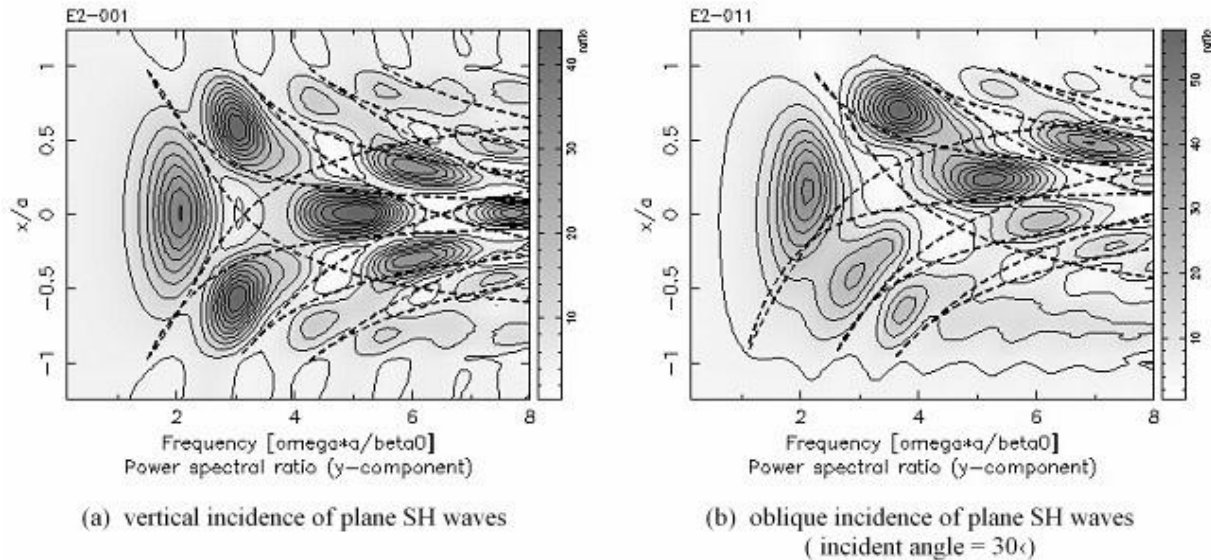


Figure 4. Amplifications and nodal lines of interferences

The distributions of amplification nodes observed in Fig. 4 can be explained as follows. Consider the interferences among the first direct wave with travel time $t(x)$ and the surface waves generated on the valley edges $x = \mp a$ at the time $t(\mp a)$ and propagating laterally to the other edges with the phase velocities $\pm v(\omega)$. Using the theoretical phase velocities of the fundamental Love wave in the equivalent flat layer as the $v(\omega)$, the nodal lines of interferences among these waves are plotted by dashed lines in Fig. 4. These nodal lines well coincide with those observed in the amplifications. This example is limited to the cases that the first direct wave and the fundamental mode of the surface waves are predominant. However, the simple explanation like this may be helpful, especially from the engineering viewpoint, to understand intuitively the real complicated phenomena arising in the alluvial valley during earthquakes.

CONCLUSION

We have introduced and defined the equivalent flat layer model of an alluvial valley with respect to the dispersion characteristics of surface waves to quantify the degree of geometrical irregularities and their influence on ground motions. Fundamental examinations performed in this study suggest that the newly introduced geometrical index could have potential utility to characterize the ground motions in various shapes of alluvial valleys.

ACKNOWLEDGMENTS

This study was supported in part by a Grant-in-Aid for Scientific Research (No. 15710140) from the Ministry of Education, Culture, Sports, Science and Technology, Japan.

REFERENCES

1. Bard, P.-Y. and M. Bouchon “The seismic response of sediment-filled valleys. Part 1. The case of incident SH waves” Bulletin of the Seismological Society of America 1980; 70: 1263-1286
2. Bard, P.-Y. and M. Bouchon “The seismic response of sediment-filled valleys. Part 2. The case of incident P and SV waves” Bulletin of the Seismological Society of America 1980; 70: 1921-1941
3. Marsh, J., T. J. Lankin, A. J. Haines, and R. A. Benites “Comparison of linear and nonlinear seismic response of two-dimensional alluvial basins” Bulletin of the Seismological Society of America 1995; 85: 874-889
4. Matsuda, S., M. Kawano, and K. Asano “The Riccati method for seismic response analysis of alluvial valley with irregular boundary – Application to three-dimensional problem –“ Annual Reports of Kinki Branch of AIJ 2002: 325-328 (in Japanese)